



Research article

Microbial succession and denitrifying woodchip bioreactor performance at low water temperatures

Maria Hellman^{a,*}, Jaanis Juhanson^a, Felicia Wallnäs^{a,1}, Roger B. Herbert^b, Sara Hallin^a

^a Swedish University of Agricultural Sciences, Department of Forest Mycology and Plant Pathology, Box 7026, 75007, Uppsala, Sweden

^b Uppsala University, Department of Earth Sciences, Villavägen 16, 75226, Uppsala, Sweden



ARTICLE INFO

Handling editor: Raf Dewil

Keywords:

Denitrifying bioreactor
Woodchips
Denitrification
DNRA
N₂O
Microbial community

ABSTRACT

Mining activities are increasingly recognized for contributing to nitrogen (N) pollution and possibly also to emissions of the greenhouse gas nitrous oxide (N₂O) due to undetonated, N-based explosives. A woodchip denitrifying bioreactor, installed to treat nitrate-rich leachate from waste rock dumps in northern Sweden, was monitored for two years to determine the spatial and temporal distribution of microbial communities, including the genetic potential for different N transformation processes, in pore water and woodchips and how this related to reactor N removal capacity. About 80 and 65 % of the nitrate was removed during the first and second operational year, respectively. There was a succession in the microbial community over time and in space along the reactor length in both pore water and woodchips, which was reflected in reactor performance. Nitrate ammonification likely had minimal impact on N removal efficiency due to the low production of ammonium and low abundance of the key gene *nrfA* in ammonifiers. Nitrite and N₂O were formed in the bioreactor and released in the effluent water, although direct N₂O emissions from the surface was low. That these unwanted reactive N species were produced at different times and locations in the reactor indicate that the denitrification pathway was temporally as well as spatially separated along the reactor length. We conclude that the succession of microbial communities in woodchip denitrifying bioreactors treating mining water develops slowly at low temperature, which impacts reactor performance.

1. Introduction

Nitrogen (N) pollution is a major threat to ecosystems and supports emissions of the greenhouse gas nitrous oxide (N₂O). The problem is mainly caused by the widespread use of fertilizers, but an additional, increasingly recognized N source is nitrate originating from undetonated explosives used during mining activities (Baily et al., 2013). Mitigating nitrate pollution from mining activities is a challenge due to the large volumes of water and diffuse leaching of nitrate from waste rock dumps. Fixed-bed denitrifying bioreactors based on woodchips for treating agricultural drainage (Schipper et al., 2010) have recently been employed to treat nitrate-rich mining water (Nordström and Herbert, 2018). During operation, nitrate is effectively removed through the anaerobic microbial process denitrification (Nordström and Herbert, 2018; Robertson and Cherry, 1995; Schipper and Vojvodić-Vuković, 2000) where nitrate is converted to dinitrogen gas. However,

dissimilatory reduction of nitrate to ammonium (DNRA) also reduces nitrate, but to ammonium, thereby retaining N in the system (Kraft et al., 2014) and competition between denitrification and DNRA can develop (Nordström et al., 2021). Further, N₂O can be released if the denitrification process is incomplete (Philippot et al., 2011), which is common among denitrifying microorganisms (Graf et al., 2014). Thus, competing N-transforming processes can take place in the anoxic environment of the bioreactor, but the prevalence and importance of these processes have rarely been considered (Aalto et al., 2020; McGuire et al., 2023; Nordström and Herbert, 2018).

Efforts have been made to optimize process performance and bioreactor design by considering reactor hydraulics (Hoover et al., 2016; Martin et al., 2019; Nordström and Herbert, 2017; Schaefer et al., 2021), redox state (McGuire et al., 2023), substrates for the denitrifying microorganisms (Cameron and Schipper, 2010; Hellman et al., 2021; McGuire et al., 2021; Wang and Chu, 2016) and choice of inoculum

* Corresponding author.

E-mail addresses: Maria.Hellman@slu.se (M. Hellman), jaanis.juhanson@slu.se (J. Juhanson), felicia.wallnas@semcon.com (F. Wallnäs), roger.herbert@geo.uu.se (R.B. Herbert), sara.hallin@slu.se (S. Hallin).

¹ Present address: Semcon, Rapskatan 7E, 754 40 Uppsala, Sweden.

<https://doi.org/10.1016/j.jenvman.2024.120607>

Received 9 November 2023; Received in revised form 8 February 2024; Accepted 10 March 2024

Available online 26 March 2024

0301-4797/© 2024 The Authors. Published by Elsevier Ltd. This is an open access article under the CC BY license (<http://creativecommons.org/licenses/by/4.0/>).

(Lefèvre et al., 2013). Not until recently has interest been drawn to the microbial communities in the bioreactors (e. g. Aalto et al., 2020; Griefmeier et al., 2017; Jéglot et al., 2021; McGuire et al., 2023). However, few bioreactors have been investigated for community composition over longer periods of time (Nordström et al., 2021; Porter et al., 2015), despite an expected longevity of 10 years or more (Long et al., 2011; Robertson et al., 2008). Less is also known about the establishment of the N-transforming microbial communities, although reports show that the dynamics of the dominating N-transformation processes affect reactor performance (Hellman et al., 2021; Nordström et al., 2021).

Our aim was to evaluate the performance and microbiology of a denitrifying bioreactor treating N-polluted mining water during the first two years of operation. Reactor performance included overall N removal capacity, pore water chemistry in space and time within the reactor and N₂O and methane (CH₄) emissions from the reactor surface. Here we assumed that overall N removal would be controlled by the degradation of woodchips, which would be reflected by the concentration of dissolved organic carbon (DOC) in the reactor water. Further, we analyzed the development of spatial and temporal patterns in microbial communities, including their genetic potential for the N-transforming processes denitrification, N₂O reduction, and DNRA, in the pore water and woodchips. We anticipated a succession of microbial communities with a gradual development towards a complete denitrifying community (Hellman et al., 2021), both along the length of the reactor and over time. Accordingly, production of the denitrification intermediates nitrite and N₂O were expected to decrease with distance from inlet and between the years. With this work we add knowledge to the temporal and spatial development of microbial communities in a woodchip-based denitrifying bioreactor over a long time period, thereby increasing the understanding of the microbial dynamics underpinning reactor performance.

2. Material and methods

2.1. Bioreactor construction and operation

The denitrifying woodchip bioreactor was built in the sub-surface at the Kiruna iron ore mine located in northern Sweden (67°51' N, 20°13' E) in 2018 to treat nitrate-rich leachate from waste rock dumps. The bioreactor was constructed as a 2.1 m deep oblong excavation with trapezoidal cross section, 44 m × 7 m at the ground surface and 34 m × 2 m at the bottom, lined with an impermeable 1.5 mm thick HDPE plastic geomembrane. The trench was filled with decorticated pine woodchips to a height of 1.7 m above the bottom and inoculated with activated sewage sludge (in total 2 m³ of a 10:1 water:sludge slurry was

sprinkled on the woodchips during filling). The total saturated volume of the bioreactor was 217 m³. The woodchips were covered with a 0.4 m thick layer of soil (glacial till) to prevent intrusion of oxygen into the bioreactor and the whole construction was covered with a peat layer (1 m) for insulation.

To direct the flow to the deeper regions of the bioreactor, two vertical inner walls, extending from the surface to a depth of 1.1 m, were placed at 5 m from each end of the bioreactor. At the inlet side of the first inner wall, the woodchips layer was 2.1 m thick (no glacial till) and at the outlet side of the second inner wall, the compartment was filled with crushed rock (16–32 mm) to distribute the flow over the width of the bioreactor and prevent channeling (Fig. 1). Via a pumping well, 26 m upstream the bioreactor inlet, water was pumped to the bioreactor from a subsurface water reservoir (approximately 630 m³, filled with 100–200 mm crushed rock to prevent freezing) that collected leachate from a nearby waste rock pile. To maintain flows up to 0.5 L s⁻¹ in 2020, additional water was pumped from an adjacent ditch receiving leachate from the waste rock pile and likely also some surface water and groundwater. The water entered the reactor through a perforated pipe, 1.6 m above the bottom of the bioreactor, and flowed by gravity until it reached the outlet compartment where it discharged through a pipe leading to an outlet monitoring chamber. The outlet monitoring chamber contained an H-flume for determining the water discharge. An FDU90 ultrasound sensor (Endress + Hauser AG, Reinach, Switzerland) registered the water depth in the H-flume and flow was calculated from calibration data. Water temperature was continuously monitored in the pump well using a combined conductivity-temperature-water depth sensor (model CTD-10, Decagon Devices, WA, USA) and in the reactor bed, 7 m upstream from the outlet, using a temperature sensor (model DS18B20 Maxim Integrated, CA, USA).

Pipes for sampling of pore water were installed at two depths, allowing for sampling at the bottom of the reactor and from 1 m above the bottom, along the length of the bioreactor, at 3.1, 11.4, 20.5, 29.2 and 37.5 m from the inlet (Fig. 1). The lower 50 cm of the pipes were screened to allow flow. Three vertical wells for sampling of woodchips (“woodchip wells”) were installed at 4.6, 19.0 and 36.3 m from the inlet in the center of the cross section of the bioreactor through the depth of the woodchip bed. The sampling wells were 30 cm in diameter and lined with a plastic net with ca 40 × 40 mm meshing for minimal disturbance of the water flow. Within the woodchip wells, nine fine mesh cylinders (2.8 × 2.8 mm meshing; 2.5 m long and 8 cm in diameter) filled with woodchips were attached to the sides. Six anchors (0.5 m diameter) for static gas chambers were installed on the reactor surface (extending ca 0.35 m below the peat surface) and were evenly distributed over the whole surface area of the bioreactor to measure fluxes of N₂O and CH₄ using the static gas chamber technique as described (Nordström and

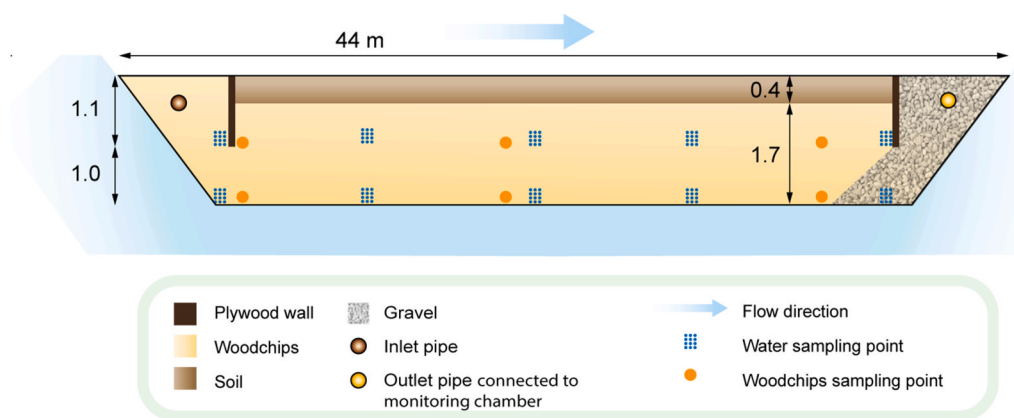


Fig. 1. Schematic illustration of the bioreactor. The distances for the sampling points are distances from the inlet pipe. Length and depth scales are not proportional to each other. The vertical pipes and well constructions for water and woodchip sampling at the indicated depths are not shown. The insulating peat layer is not shown.

Herbert, 2018). In 2019, one of the chamber anchors was placed on the surface close to the outlet pipe in the gravel-filled outlet compartment of the bioreactor, to serve as a non-woodchip control, but was moved to the bioreactor surface 2020.

Bioreactor operation started September 17, 2018, but the first and second year will be referred to as 2019 and 2020 respectively since they were full operational years. The discharge was monitored automatically via the water level in the H-flume in the outlet monitoring chamber from June 28, 2019. The flow varied between 0.12 and 1.07 L s⁻¹ (2019, n = 5709, mean flow 0.37 L s⁻¹) and 0.21 and 0.64 L s⁻¹ (2020, n = 2017, mean flow 0.39 L s⁻¹) during the sampling periods. Based on an average flow of 0.37 L s⁻¹, the theoretical hydraulic residence time (HRT) in the bioreactor was ca. 3.7 days. Nitrogen in the inlet water was entirely in the form of nitrate with the average concentrations 84.1 ± 19.4 (mean ± SD; n = 17), 61.1 ± 16.6 (n = 43) and 36.9 ± 10.4 (n = 27) mg N L⁻¹ during 2018, 2019 and 2020, respectively (Fig. 2a–c). The concentration of dissolved organic carbon (DOC) in the inlet water was 3.48 ± 1.38 (mean ± SD, n = 16); 2.92 ± 1.16 (n = 46); 5.57 ± 2.19 (n = 27) mg L⁻¹ in 2018, 2019 and 2020, respectively (Fig. 2d). Alkalinity, pH, conductivity, concentrations of major ions and copper, nickel, lead, and zinc ions are found in Table S1. The mean water temperature in the pumping well was 3.0 °C in 2019 and 3.4 °C in 2020 (n = 136 and 171, respectively). In the reactor bed, the mean temperature was 3.2 °C both years

(n = 171 and 164, respectively).

2.2. Sampling of water, woodchips, and gas emitted from the surface

Water for analyses of nitrate, nitrite, ammonium, and total N was collected twice a week October–December 2018, May–November 2019, and March–October 2020 from the pumping well and outlet monitoring chamber and approximately once per month in the summer periods 2019 and 2020 from the pore water sampling pipes. Water for microbial analyses was collected from the pumping well, the monitoring chamber, and the pore water pipes five times in 2019 and three times in 2020. Water from the outlet chamber was collected directly in a beaker, whereas samples from the pumping well and from the pore water pipes were collected using a peristaltic pump. Circa 2 L of water was discarded before collection of 2 L. Water for microbial analyses was filtered through a 0.22 µm pore size Sterivex® filter until clogged, with a mean filtered volume of 1.4 L. The filters were kept at -20 °C until analysis.

For analysis of dissolved gases in the inlet (pumping well) and outlet (monitoring chamber), water was sampled by fully immersing an open 50 mL plastic syringe in the water, capping it with the piston and a stopper plug while still under water, and subsequently injecting 50 mL of water into sealed 118 mL glass bottles containing 1 mL ZnCl₂ (50 % w/v) and 1 atm of air (2019) or N₂ (2020). At equilibrium, 50 mL

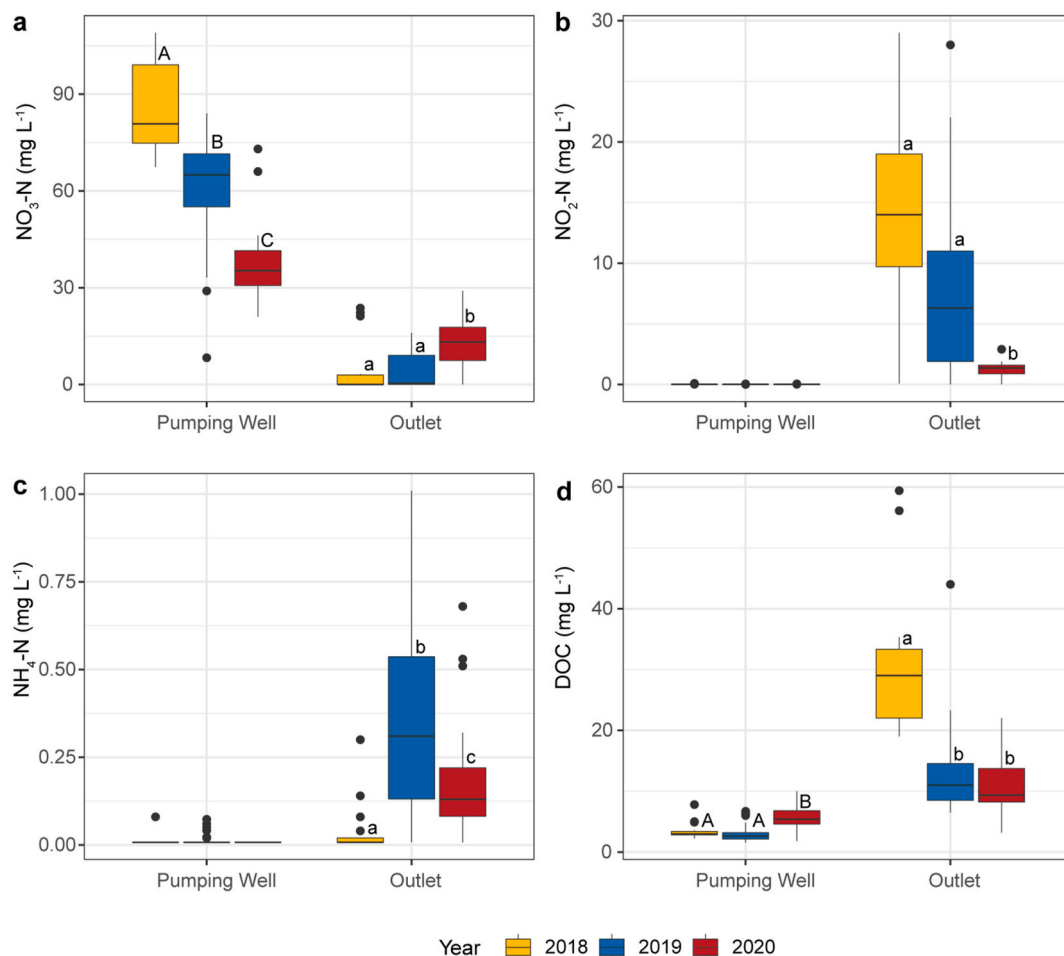


Fig. 2. Concentration of nitrogen species and dissolved organic carbon in the pumping well with inlet water and the outlet monitoring chamber of the bioreactor 2018–2020. a) nitrate, b) nitrite, c) ammonium, and d) dissolved organic carbon. Samples below detection limit (for nitrate 0.23 mg N L⁻¹ and for nitrite and ammonium 0.015 N mg L⁻¹) were assigned a value of half the detection limit. Box limits represent the interquartile range with median values represented by the center line. Whiskers represent values ≤ 1.5 times the upper and lower quartiles, while points indicate values outside this range. Different capital and lower-case letters above boxes indicate significant differences across samples in the pumping well and outlet, respectively, (Dunn's test, p < 0.05). n = 13–17 (2018), 45–50 (2019) and 26–28 (2020).

headspace gas from the 118 mL glass bottles was flushed through 22 mL vials to completely replace the air in the vials with headspace gas.

Woodchips for microbial analyses were sampled five times in 2019 and three times in 2020, within one day from the water sampling for microbial analyses, by removing one of the woodchip-filled mesh cylinders from a woodchip well and collecting six 10 cm length samples of the cylinder, representing 0–10; 10–20; 20–30; 100–110; 110–120 and 120–130 cm from the bottom of the bioreactor. The remaining woodchips were put back into the reactor bed. The samples were first kept at $-20\text{ }^{\circ}\text{C}$ and later freeze-dried.

For determining N_2O and CH_4 fluxes from the surface of the reactor, gas samples were collected as described in Nordström and Herbert (2018). From each of the static gas chambers nine sets of samples were collected in 2019 and three sets in 2020.

2.3. Chemical analyses of water and gas

Concentrations of nitrate, nitrite, and ammonium in the pore water and from the monitoring wells were photometrically determined using the Hach LCK Cuvette Test System (Hach Lange GmbH, Düsseldorf, Germany). Total N and DOC concentrations were determined in the samples from the monitoring wells using the Swedish Standard methods EN-12260:2004 and EN-1484 respectively.

Percentage of N removal (N removal efficiency) was calculated as $100 \times ([\text{total N}_{\text{in}}] - [\text{total N}_{\text{out}}]) / [\text{total N}_{\text{in}}]$. Nitrogen load was calculated as $([\text{total N}_{\text{in}}] - [\text{total N}_{\text{out}}]) \times Q$ where [total N] is the concentration of total N in the water from the pumping well and outlet monitoring chamber, respectively and Q is the flow. Nitrogen removal rate was calculated as the N load divided by the total saturated volume of the bioreactor.

All gas samples were analyzed for N_2O and CH_4 by gas chromatography (Clarus 500 GC, PerkinElmer, Waltham, MS, United States) using an electron capture- and flame ionization detector for N_2O and CH_4 , respectively. Dissolved gas concentrations were determined via headspace equilibrium using the general gas law and the temperature-dependent Bunsen coefficient, without correcting for the increased pressure in the sampling bottles (Supplementary methods). The accumulated gas concentrations from the surface were recalculated to flux rates using the R package HMR v. 1.0.1 (Pedersen, 2020).

2.4. DNA extraction and quantitative PCR

The Sterivex filters were detached from the filter cartridges and DNA from the water samples was extracted from the filters using the DNeasy PowerLyzer PowerSoil kit (Qiagen GmbH, Hilden, Germany). The amount of glass beads and the volumes of the reagents were modified (Supplementary methods). DNA from the woodchip samples was extracted using a combination of extraction chemistry from the DNeasy Plant Maxi kit (Qiagen GmbH, Hilden, Germany) and further purification using the Macherey-Nagel Nucleospin Soil kit (Macherey-Nagel GmbH & Co, Düren, Germany). For each sample, two separate extractions from 4 g of woodchips were combined at the end of the extraction protocol. Reagent volumes were modified (Supplementary methods).

Quantitative PCR was used to estimate the size of the total bacterial community by quantifying the 16S rRNA gene abundance (Muyzer et al., 1993). The functional genes *nirS* (Throbäck et al., 2004) and *nirK* (Henry et al., 2004), *nosZI* (Henry et al., 2006) and *nosZII* (Jones et al., 2013), *hdh* (Schmid et al., 2008), and *nrfA* (Mohan et al., 2004; Welsh et al., 2014) were used to determine the genetic potentials for denitrification, N_2O reduction, anammox, and DNRA. Each qPCR reaction contained 3 ng (water samples) or 1 ng (woodchip samples) template DNA, iQSYBRGreen Supermix (BioRad, Hercules, CA, United States), 15 μg Bovine Serum Albumin (BSA), and primer concentrations of 0.5–2.0 μM in a total volume of 15 μL . Two separate PCR runs were performed for each sample using the BioRad CFX or 384 Real-Time Systems. Thermal cycling conditions, primer sequences, and concentrations are available

in Table S2. Standard curves were obtained using serial dilutions of linearized plasmids containing cloned fragments of the respective genes. Potential PCR inhibition was tested as described in Hellman et al. (2021) and no inhibition was detected for the DNA concentrations used.

2.5. Sequencing and bioinformatic analyses of 16S rRNA genes

Part of the V3–V4 region of the 16S rRNA gene was sequenced to determine the composition and diversity of the bacterial and archaeal communities in the water and the woodchips using a two-step amplification protocol. The first step was performed in duplicate 15 mL reactions containing 4 ng template DNA, 0.25 mM of primers pro515f and pro926r (Quince et al., 2011; Parada et al., 2016) with Nextera adaptor-sequences (Illumina Inc., San Diego, CA, United States), 15 μg BSA and 1 \times Phusion® HighFidelity PCR Master Mix (New England Biolabs, Ipswich, MA, USA). Amplicons from the duplicate reactions were pooled and purified using Sera-Mag™ magnetic beads (GE Healthcare, Chicago, IL, USA). The second step was performed in duplicate 30 mL reactions with 10 % of the final purified product from the first step as template and 0.20 mM of primers with Nextera adapter- and barcoding regions for dual labelling of the fragments. The duplicate reactions were pooled, inspected on agarose gel, purified as above, and quantified using the Qubit® fluorometer (Thermo Fisher Scientific, Waltham, MA, USA). Equal amounts of purified amplicons were pooled, the quality of the pool was checked on the Bioanalyzer and the pool of libraries was sequenced by SciLifeLab in Uppsala on an Illumina MiSeq instrument using the 2×250 bp chemistry. The raw sequence dataset is available under BioProject accession number PRJNA1035505.

The 16S rRNA sequences were processed as described in Hellman et al. (2022), except that the non-redundant reference database SILVA version 138 was used to classify representative OTUs. SINA (Pruesse et al., 2012) was used to align nucleotide sequences of the representative OTUs to the SILVA database, and FastTree (Price et al., 2009) with the Jukes-Cantor and CAT model (Jukes and Cantor, 1969) was used to construct a phylogenetic tree from the aligned sequences. Mitochondrial and chloroplast reads were identified and removed, resulting in 10,123 OTUs in the dataset. After rarefying the dataset at the depth of 10,015 sequences per sample 8954 OTUs remained. For subsequent analyses, the dataset was divided into woodchips and water samples, respectively.

2.6. Statistical analyses

Statistical analyses were performed using R version 4.1.2 (R Development Core Team, 2021). Water chemistry, gene abundance and phylogenetic diversity data did not meet the requirements for normality, hence for comparisons between two groups Wilcoxon rank sum test was used and for comparisons between more than two groups we used Kruskal–Wallis test followed by Dunn’s test, for pairwise contrasts. Student’s *t*-test was used where data met the requirements for normality. Corrections for multiple comparisons were done by false discovery rate (Benjamini and Hochberg, 1995). Spearman’s rank-order correlation was used to test the relationship between DOC and N removal efficiency. Since there were no depth-related differences in nitrate concentration, functional gene abundance or phylogenetic diversity across the year per sampling location (Wilcoxon rank sum test, $p > 0.05$), data from the two depths were merged in the statistical analyses. For the ordinations, data from the two depths were handled separately.

Frequently distributed OTUs were determined separately for water and woodchips samples, as described in Hellman et al. (2022) and Saghaei et al. (2022), resulting in 755 and 1608 core OTUs in the woodchips and water samples, respectively that retained 88.2% and 93.3% from the total OTU abundances in respective datasets (Table S3). Phylogenetic diversity (Faith, 1992) of the communities was estimated using *estimate_pd* function in “btools” package. Nonmetric multidimensional scaling (NMDS) of the unweighted Unifrac phylogenetic distances was used to visualize community patterns with “phyloseq” and “ggplot”

packages, and function *envfit* in “vegan” package to correlate N cycling gene abundances with the community structure. PERMANOVA and ANOSIM (functions *adonis* and *anosim*) analyses were used to test the differences in community composition between different grouping categories. Differential abundance analyses of the core OTUs were performed using ALDEx2 (Fernandes et al., 2013) and visualized using iTOL (Letunic and Bork, 2007).

3. Results

3.1. Reactor performance and water chemistry

The total N load varied between 0.8 and 2.5 kg day⁻¹. Despite a higher incoming nitrate concentration in 2019 (Fig. 2a), the load in 2020 was relatively similar due to a higher flow. In average, 79.7 ± 12.8 (mean ± SD; n = 32) and 64.7 ± 22.0 (n = 30) % of the total N was removed in 2019 and 2020, respectively and the N removal efficiency correlated with the outlet DOC concentration (Spearman’s rank correlation, p < 0.05, 2019 and 2020, both when tested separately and combined; Fig. 3). The slopes were similar despite different N removal capacities. The removal rate was significantly higher in 2019, where the average removal was 5.59 ± 1.88 compared to 3.85 ± 1.64 g N day⁻¹ m⁻³ (saturated bed volume) in 2020 (t-test p < 0.001, n = 32 and 30, respectively). The bioreactor released similar concentrations of DOC in 2019 and 2020, but they were significantly higher in 2018 when reactor operation started than the following years (Dunn’s test; Fig. 2d).

In the pore water, the temporal variation of N species per sampling point was lower in 2020 compared to the first two years. Nitrate concentrations decreased with distance from the inlet, with the most rapid decrease the first year (Fig. S1a). However, nitrite was produced in the first part of the bioreactor and the change in concentration along the length of the reactor showed different patterns between the two sampling depths and years, with the highest concentrations in 2018 and 2019 (Figs. S1b and c). In contrast to the production of nitrite, ammonium production was higher towards the end of the bioreactor (Fig. S1d), with the highest concentrations in 2019 and 2020. Thus, both nitrite and ammonium were formed in the bioreactor and were also released with the outlet water (Fig. 2).

3.2. Greenhouse gases

The concentration of N₂O in the water decreased during reactor passage in 2019, from 214 ± 61 mg m⁻³ in the inlet to 140 ± 123 mg

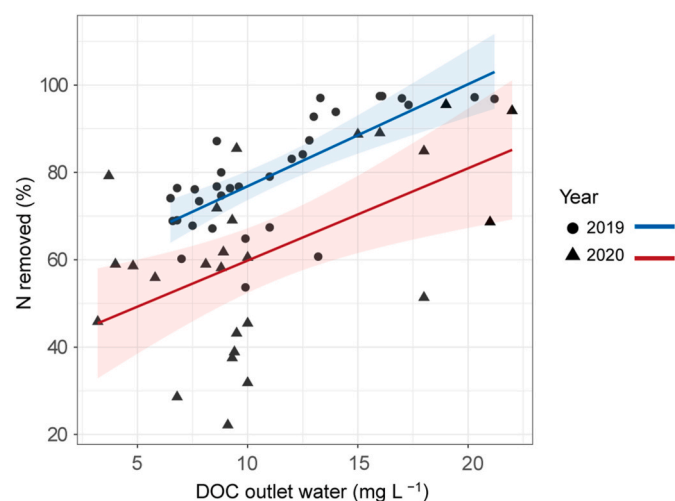


Fig. 3. Nitrogen removal efficiency as a function of concentration of dissolved organic carbon (DOC) in the outlet water in 2019 (blue line) and 2020 (red line).

m⁻³ in the outlet water (t-test p = 0.027) with the largest reductions, 97–98 %, in June and September. By contrast, the samples from 2020, indicate net production of N₂O in the reactor (Fig. 4a and b). The dissolved N₂O–N leaving the bioreactor was in 2019 less than 0.5 % of the reactive N load and on the one occasion measured in 2020, dissolved N₂O–N constituted 1.6 % of the N load. Emissions of N₂O from the reactor surface were highest in the middle of the summer periods and across the whole season, there was no difference between emissions in 2019 and 2020, with mean fluxes of 9.5 and 6.6 mg N₂O m⁻² day⁻¹ respectively, corresponding to 1.5 and 1.0 g N day⁻¹ from the reactor surface area. However, when comparing between corresponding dates, the flux was significantly lower in 2020 (Fig. 4c and d). The N₂O fluxes varied over the reactor surface, as did the relative contribution from each of the six sampling chambers in both years. In general, lower emissions were detected in the beginning of the reactor. The flux from the control area 2019 was low, the contribution varied between 0 and 7 % (mean 2.5 %) of the total flux.

To reveal possible short-term temporal variation in N₂O emissions, sampling was done five consecutive days in the beginning of July 2019 (Fig. 4c). Across the week, no significant differences in flux per day over the whole surface were detected. Thus, location was more important than the time of sampling.

Methane was not detectable in the inlet water in 2019. By the small adjustment in sampling procedure, the detection limit was substantially lowered in 2020, and low concentrations of CH₄ (0.74 ± 0.26 mg m⁻³) were found in the inlet water. After passage through the bioreactor, the levels had increased to 5–10 mg m⁻³, indicating production of CH₄ in the reactor in both years. However, the fluxes of CH₄ from the reactor surface were neglectable, and in most cases indicated a consumption rather than an emission of CH₄.

3.3. Functional gene abundances and size of total bacterial communities

For the abundance of functional genes, different patterns were observed along the bioreactor between years in the water and in the woodchips (Fig. S2). In the water, with the exception for *nirK*, the absolute abundance of genes decreased between 2019 and 2020, whereas in the woodchips an increase was observed (Figs. S2a–j). The abundance of the 16S rRNA gene, proxy for the size of the total bacterial community, did not change between years in the woodchips, but in the pore water there was a decrease at all sampling locations except at 42.5 m from the inlet (Wilcoxon test per sampling position; Fig. S2k and l). The relative gene abundances in both sample types, with the exceptions of *nosZ* clade I and II and *nrfA* in the water, increased 2020 (Wilcoxon test, all samples per year and sample type included; Table S4).

The ratio between genes indicating N₂O production (sum of *nir* genes) and reduction (sum of *nosZ* genes) was predominantly lower than 1 in both water and woodchips, suggesting a genetic net potential for N₂O reduction (Fig. 5a and b) and complete denitrification. Furthermore, there were spatial patterns showing higher ratios closer to the inlet of the reactor (Fig. 5a and b). In 2019, the ratio between the abundances of *nrfA* and sum of *nir* genes increased towards the end of the reactor in both water and woodchips, suggesting an increased importance of DNRA along the reactor, but this was not detected in 2020 (Fig. 5c and d). The marker gene for anammox was not detected in the bioreactor at any location and occasion.

3.4. Microbial community structure, diversity, and composition

The microbial community composition of frequent OTUs was different between water and woodchips samples (permanova p < 0.005, anosim p < 0.005). Within the water and woodchips samples, community composition was affected by year, but also by distance from the inlet, and sampling depth (permanova p < 0.005, p < 0.05 and p < 0.05, respectively) (Fig. 6a and b). The separation of communities between years in both water and woodchip samples correlated with the *nrfA/nir*

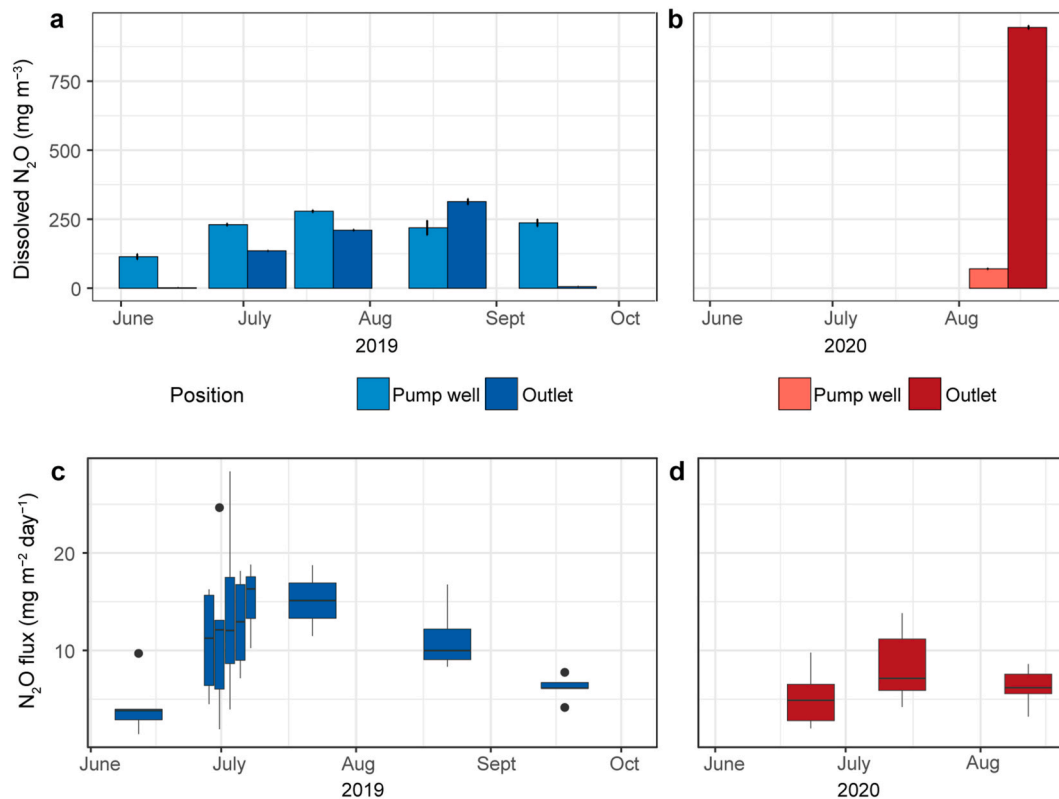


Fig. 4. Nitrous oxide released from the reactor 2019 and 2020. a) and b) Concentrations of dissolved N₂O in the pumping well with inlet water and the outlet monitoring chamber of the bioreactor. Error bars show ± 1 standard deviation, $n = 3\text{--}4$. c) and d) Fluxes of N₂O from the surface of the bioreactor. Box limits represent the inter-quartile range with median values represented by the center line. Whiskers represent values ≤ 1.5 times the upper and lower quartiles, while points indicate values outside this range, $n = 2\text{--}5$, data from the control measuring point not included.

gene abundance ratio, while the *nir/nos* gene ratios correlated with the separation of microbial communities along the reactor length (Fig. 6). In woodchips, the separation of microbial communities between years correlated with the *nosZI/nosZII* gene ratio, while *nrfA/nir* ratio correlated with the separation of communities along the reactor (Fig. 6b).

The phylogenetic diversity (Faith's PD) was in general higher in the water samples compared to the woodchips (47.2 ± 11.6 , $n = 95$, and 33.7 ± 9.6 , $n = 44$, respectively, Wilcoxon rank sum test $p < 0.05$), and higher in 2020 compared with 2019 (50.3 ± 8.4 , $n = 52$, and 38.5 ± 12.8 , $n = 87$, respectively, Wilcoxon rank sum test $p < 0.05$), except for the water from the pumping well, which demonstrated higher phylogenetic diversity than then woodchips in 2019 (66.8 ± 2.2 , $n = 4$, and 54.4 ± 2.1 , $n = 3$, respectively, Wilcoxon rank sum test $p < 0.05$) (Table S5). The phylogenetic diversity changed along the distance of the bioreactor (Kruskal-Wallis' test $p < 0.05$) and generally decreased with increasing distance in both water and woodchips samples, especially in 2019, and the decrease was fastest in the beginning of the bioreactor (Table S5). The phylogenetic diversity in the water samples from 2020 was more consistent along the distance from the inlet of the reactor, except for the samples from 3.1 m from the inlet that differed from those 29.2 and 37.5 m from the inlet pump (Dunn's test with false discovery rate adjusted p -values, $p < 0.05$). Sampling depth did not influence the phylogenetic diversity in neither the water nor the woodchips.

The microbial communities in both water and woodchips were dominated by Proteobacteria, Actinobacteriota, Bacteroidota, Firmicutes and Verrucomicrobiota, but the dynamics of their relative abundance varied along the distance from the inlet and between years (Fig. S3). In the woodchips, Actinobacteriota, Alphaproteobacteria and Verrucomicrobiota decreased along the distance from the inlet in both 2019 and 2020. However, their relative abundances were higher in 2020, while Bacteroidota and Firmicutes increased along the distance

from the inlet in both years, although the relative abundance of both phyla were lower in 2020 (Fig. S3a and b, S4). The abundance of the phylum Desulfobacterota was highest in the woodchip samples most distant from the inlet (36.3 m), which was also reflected by the corresponding water sample (37.5 m). For the dominant phyla, changes in abundances along the reactor were similar between the two sample types in 2019. By contrast, changes in relative abundances of e.g. Bacteroidota and Alphaproteobacteria in the woodchips were not reflected in the water samples in 2020 (Fig. S3c and d, S4). The phylum Patescibacteria increased substantially in the water 2020, particularly in the middle section of the bioreactor. Unlike in woodchips, the abundance of Verrucomicrobiota was lower in the water samples in 2020 compared with 2019.

4. Discussion

The bioreactor removed N from the waste-rock leachate during the entire period, but with lower efficiency and removal rate during the second operational year. A decreasing efficiency over time has been observed in other denitrifying woodchip bioreactors (Addy et al., 2016; David et al., 2016) and has been attributed to the availability of DOC (David et al., 2016; Hassanpour et al., 2017). DOC concentration is typically high at start-up, but decrease over time (Nordström and Herbert, 2018; Warneke et al., 2011). As anticipated, the decreasing N removal in the bioreactor studied agrees with the observed yearly decrease in DOC in the outlet water. The start-up phase and the first full year of operation were also characterized by a considerable production of nitrite in the reactor, with high concentrations also detected in the effluent, similar to what has been shown in other studies (Warneke et al., 2011; Herbert et al., 2014; Hellman et al., 2021). The initial nitrite production and the increase in relative abundance of the denitrification

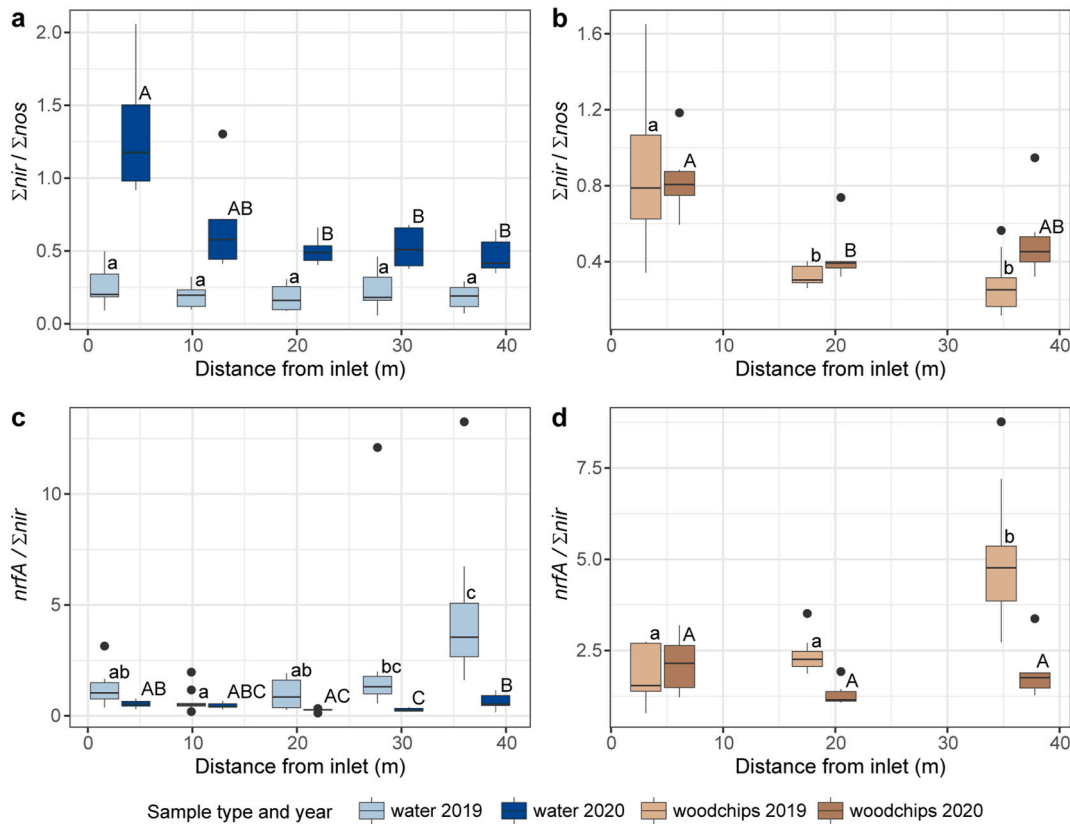


Fig. 5. Ratios between abundance of genes along the length of the bioreactor in water (left side) and woodchip (right side). a) and b) sum of *nirS* and *nirK* divided by sum of *nosZI* and *nosZII*, c) and d) *nrfA* divided by sum of *nirS* and *nirK*. Box limits represent the inter-quartile range with median values represented by the center line. Whiskers represent values ≤ 1.5 times the upper and lower quartiles, while points indicate values outside this range. $n = 10$ (2019) and 6 (2018). Different lower-case and capital letters above boxes indicate significant differences across samples 2019 and 2020, respectively, (Dunn's test, $p < 0.05$).

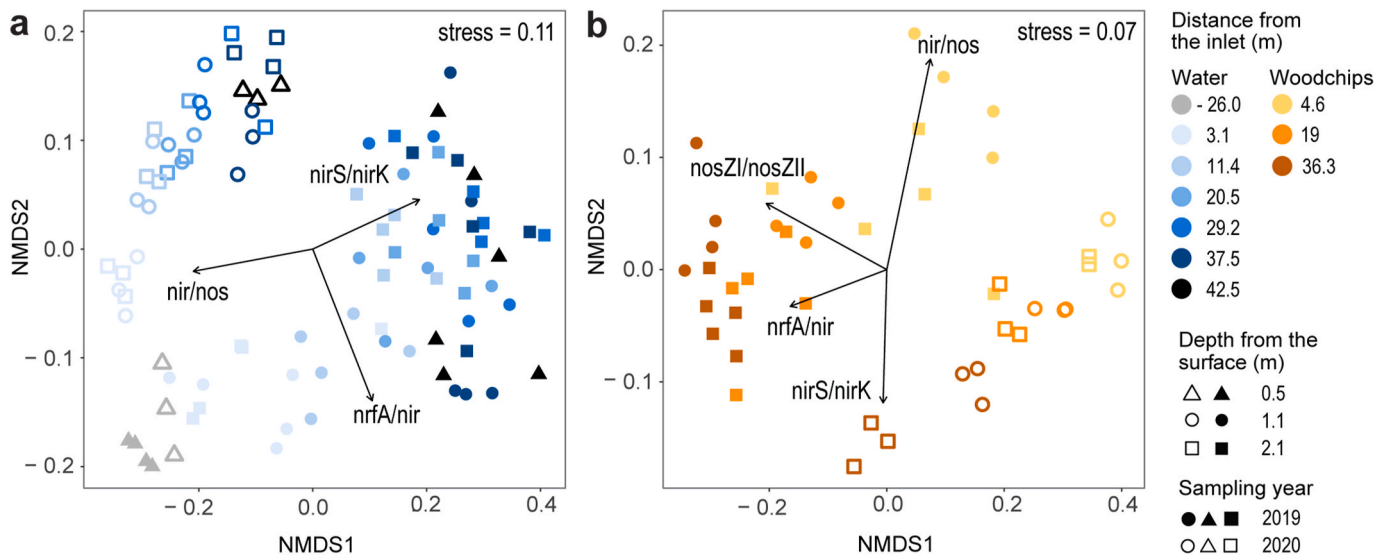


Fig. 6. Microbial community composition in the a) water and b) woodchip samples along the bioreactor during two years of operation. For the water samples, -26.0 and 42.5 m from the inlet refer to pumping well water and outlet water, respectively. Ordinations are based on non-metric multidimensional scaling (NMDS) of unweighted Unifrac distances using rarefied frequent OTUs. Significant ($p < 0.05$) correlations between ordination axis and the abundance ratios of N cycling genes are shown as vectors which lengths are proportional to the strength of the correlations.

genes in the woodchips the second year suggest a slow development of a sufficient and more complete denitrifying community, in agreement with our hypotheses. Further, when normalizing the gene abundances to the number of 16S rRNA genes, the fraction of denitrification genes in

the overall bacterial community was higher the second year, which shows that there is not just a general increase of microorganisms in the woodchips but an enrichment of denitrifiers. This pattern coincided with a higher ammonium production and a higher *nrfA/nir* ratio in 2019

compared to 2020, indicating that DNRA could play a larger role before the denitrifying community is fully developed. Nevertheless, the production and release of ammonium from the bioreactor had a negligible contribution to the total release of N. Thus, we conclude that DNRA had minimal impact on the overall N removal efficiency, which agrees with a previous study on the treatment of waste rock leachate (Nordström et al., 2021).

There was not only a change in the N cycling communities over time but also in space along the reactor, which was reflected in the genetic potential for N cycling, water chemistry, and ultimately also reactor performance. In contrast to the findings by Herbert et al. (2014), we only found minor effects of reactor depth on water chemistry and abundances of N-transformation guilds. Similar to what was observed over time, a more complete denitrification process also seemed to develop along the reactor length, as indicated by a decreasing ratio between *nir* and *nos* genes with distance from the inlet. This pattern coincided with the increased nitrate reduction and lower concentrations of intermediate N species like nitrite. Altogether, our results indicate that the denitrification pathway was spatially separated along the reactor and that unwanted reactive N species were produced at different locations in the reactor, especially during the first year of operation.

Nitrogen also left the bioreactor in the form of N_2O , dissolved in the outlet water and emitted from the reactor surface. However, in relation to the influent nitrate concentration, the amount of dissolved N_2O discharged was low. This is supported by the genetic potential for complete denitrification, showing a higher capacity for N_2O reduction than production, in the denitrifying communities present in both the pore water and woodchips. Less N_2O per day left the bioreactor via direct emissions from the surface than dissolved in the effluent, which has also been noted from other denitrifying woodchip systems (Davis et al., 2019; Warneke et al., 2011). However, the emissions of N_2O from the surface did not necessarily reflect the production of the gas in the bioreactor compartment since the surface of the reactor was covered with peat. The purpose of the peat layer was to insulate the reactor bed, but it might also have functioned as a N_2O sink if nitrous oxide reducing microorganisms in the peat layer used the gas produced in the bioreactor. In agreement, covering the reactor surface with soil has proven a way of mitigating N_2O losses from the surface (Christianson et al., 2013; Manca et al., 2021). The N_2O fluxes from the bioreactor were higher than those from fertilized agricultural soils. Fluxes from soils estimated based on the N_2O emission factor (EF) range 0.2–1.8 % (different fertilizer forms and climates, IPCC, 2019) and at a fertilization rate of 100–120 kg N year⁻¹ and ha⁻¹ the emissions are 8–60 times lower than those from the bioreactor surface. However, considering that the area of a single bioreactor is less than 300 m², the overall contribution to global N_2O emissions would be small. The potential contribution of N_2O emitted from the bioreactor applying the indirect N_2O EF on the nitrate load of the reactor was also estimated. Using an EF of 0.6 % (Tian et al., 2019), the modelled release of N_2O was 0.17 kg N per 98 days and 0.09 kg per 52 days in summers 2019 and 2020, respectively, which is similar to the measured fluxes (0.21 and 0.07 kg N respectively during the same periods). Overall, our results indicate that the use of denitrifying woodchip bioreactors for remediation of nitrate polluted mining wastewater does not increase the amount of N_2O released to the atmosphere. However, at the highly reduced conditions occurring when the bioreactor water is depleted of nitrate, there is a risk that CH_4 is produced by methanogenic archaea (Conrad, 2020). In the present study, only small amounts of CH_4 were produced in the reactor and the emission measurements suggests that the peat layer was a small sink of CH_4 , similar to drained peatlands (Andert et al., 2012).

The difference in reactor performance between the two operational years as well as along the length of the reactor coincided with differences in the microbial communities in both water and woodchips. The most abundant phyla and classes, Actinobacteria, Alphaproteobacteria, Bacteroidota, Firmicutes and Gammaproteobacteria also dominate other woodchip-based reactors for nitrate removal (e.g. Aalto et al., 2022;

Jégliot et al., 2022; McGuire et al., 2023). The microbial community in the water samples included remarkably more OTUs compared to the woodchips, indicating that many of the microorganisms present in the water did not establish in the woodchips. The higher phylogenetic diversity in the water the second year was possibly due to the additional water from a nearby pond. This was indicated by higher abundances in the reactor water of some orders within class Gammaproteobacteria (Legionellales, Coxiellales) often found in natural aquatic environments (Graelles et al., 2018). The higher N removal of the bioreactor in the first year may partially be explained by the higher abundance of some microbial taxa. For example, OTUs classified as orders Bacteroidales and Flavobacteriales, the phylum Firmicutes, and class Gammaproteobacteria (especially OTUs related to the orders Burkholderiales and Pseudomonadales) were more abundant in 2019 compared to 2020. Most of the known microorganisms from these taxonomic groups possess genes involved in different microbial N cycling pathways (*nir* and *nos* for complete denitrification, but also *nrfA* in many members from Bacteroidota and Firmicutes). Burkholderiales are identified as key denitrifiers in woodchip bioreactors (Grießmeier et al., 2021) and they also seem to play an important role in woodchip bioreactors operated under low temperatures (Jégliot et al., 2021, 2022), especially the genus *Polaromonas* (Jang et al., 2019), which were also detected in our bioreactor. Burkholderiales have been found to dominate microaerobic chemostats and can be crucial for sustaining the dissolved oxygen concentration below the threshold of sufficient N_2O reduction (Kim et al., 2022). Patescibacteria, that increased in abundance in the bioreactor in 2020, have been found to be prevalent in aquatic environments, including oligotrophic groundwater sediment (Herrmann et al., 2019) and are reported to have fermentative pathways for lactate and formate (Hosokawa et al., 2021). Fermentation processes have been proposed to be important to provide easily available C substrates for denitrifiers in woodchip bioreactors for efficient N removal (Aalto et al., 2022; Nordström and Herbert, 2018), but more work is needed to confirm this, and to determine the underlying mechanisms to help developing an optimal design and operation of denitrifying woodchip reactors treating N polluted water.

5. Conclusions

The denitrifying woodchip reactor efficiently removed nitrate from the waste rock pile leachate water, and the N removal efficiency correlated positively with the outlet DOC concentrations. Both direct and indirect N_2O emissions from the reactor were low and we conclude that woodchip denitrifying bioreactors have a minimal impact on global N_2O emissions. Initially, nitrite accumulated and DNRA was more important than denitrification for nitrate reduction, resulting in production of ammonium. However, there was a development in the microbial community towards a more complete denitrifying community along the length of the bioreactor and time, as reflected by less nitrite and decreasing N_2O concentrations in the water after bioreactor passage. Thus, the succession of microbial communities in woodchip denitrifying bioreactors is an important factor for reactor performance in both time and space.

CRedit authorship contribution statement

Maria Hellman: Conceptualization, Data curation, Formal analysis, Investigation, Methodology, Supervision, Writing – original draft, Writing – review & editing. **Jaanis Juhanson:** Data curation, Formal analysis, Investigation, Methodology, Writing – original draft, Writing – review & editing. **Felicia Wallnäs:** Formal analysis, Investigation. **Roger B. Herbert:** Conceptualization, Funding acquisition, Project administration, Supervision, Writing – review & editing. **Sara Hallin:** Conceptualization, Funding acquisition, Project administration, Supervision, Writing – original draft, Writing – review & editing.

Declaration of competing interest

The authors declare that they have no known competing financial interests or personal relationships that could have appeared to influence the work reported in this paper.

Data availability

The raw sequence dataset is available under BioProject accession number PRJNA1035505. Chemical data will be made available on request.

Acknowledgments

This work was conducted within the NITREM project, supported by EIT Raw Materials, LKAB and the Water Joint Programming Initiative and financed via the Swedish Research Council Formas (grant 2018-02788). NITREM (project number 17013) has received funding from the European Institute of Innovation and Technology (EIT). This body of the European Union received support from the European Union's Horizon 2020 research and innovation programme. Sequencing was performed by the SNP&SEQ Technology Platform in Uppsala. The facility is part of the National Genomics Infrastructure (NGI), Sweden, and the Science for Life Laboratory. The SNP&SEQ Platform is also supported by the Swedish Research Council and the Knut and Alice Wallenberg Foundation.

Appendix A. Supplementary data

Supplementary data to this article can be found online at <https://doi.org/10.1016/j.jenvman.2024.120607>.

References

- Aalto, S.L., Suurnäkki, S., von Ahnen, M., Siljanen, H.M.P., Pedersen, P.B., Tirola, M., 2020. Nitrate removal microbiology in woodchip bioreactors: a case-study with full-scale bioreactors treating aquaculture effluents. *Sci. Total Environ.* 723, 138093.
- Aalto, S.L., Suurnäkki, S., von Ahnen, M., Tirola, M., Pedersen, P.B., 2022. Microbial communities in full-scale woodchip bioreactors treating aquaculture effluents. *J. Environ. Manag.* 301, 113852.
- Addy, K., Gold, A.J., Christianson, L.E., David, M.B., Schipper, L.A., Ratigan, N.A., 2016. Denitrifying bioreactors for nitrate removal: a Meta-analysis. *J. Environ. Qual.* 45 (3), 873–881.
- Andert, J., Borjesson, G., Hallin, S., 2012. Temporal changes in methane oxidizing and denitrifying communities and their activities in a drained peat soil. *Wetlands* 32 (6), 1047–1055.
- Baily, B.L., et al., 2013. The Diavik Waste Rock Project: persistence of contaminants from blasting agents in waste rock effluent. *Appl. Geochem.* 36, 256–270.
- Benjamini, Y., Hochberg, Y., 1995. Controlling the false discovery rate - a practical and powerful approach to Multiple Testing. *Journal of the Royal Statistical Society Series B-Methodological* 57 (1), 289–300.
- Cameron, S.G., Schipper, L.A., 2010. Nitrate removal and hydraulic performance of organic carbon for use in denitrification beds. *Ecol. Eng.* 36 (11), 1588–1595.
- Christianson, L., Hanly, J., Jha, N., Saggart, S., Hedley, M., 2013. Denitrification Bioreactor Nitrous Oxide Emissions under Fluctuating Flow Conditions. *ASABE, St. Joseph, MI*, p. 1.
- Conrad, R., 2020. Methane production in soil environments-anaerobic biogeochemistry and microbial life between flooding and desiccation. *Microorganisms* 8 (6), 881.
- David, M.B., Gentry, L.E., Cooke, R.A., Herbstritt, S.M., 2016. Temperature and substrate control woodchip bioreactor performance in reducing tile nitrate loads in east-central Illinois. *J. Environ. Qual.* 45 (3), 822–829.
- Davis, M.P., Martin, E.A., Moorman, T.B., Isenhardt, T.M., Soupir, M.L., 2019. Nitrous oxide and methane production from denitrifying woodchip bioreactors at three hydraulic residence times. *J. Environ. Manag.* 242, 290–297.
- Faith, D.P., 1992. Conservation evaluation and phylogenetic diversity. *Biol. Conserv.* 61 (1), 1–10.
- Fernandes, A.D., Macklaim, J.M., Linn, T.G., Reid, G., Gloor, G.B., 2013. ANOVA-like differential expression (ALDEx) analysis for mixed population RNA-seq. *PLoS One* 8 (7).
- Graelles, T., Ishak, H., Larsson, M., Guy, L., 2018. The all-intracellular order Legionellales is unexpectedly diverse, globally distributed and locally abundant. *FEMS (Fed. Eur. Microbiol. Soc.) Microbiol. Ecol.* 94 (12).
- Graf, D.R.H., Jones, C.M., Hallin, S., 2014. Intergenomic comparisons highlight modularity of the denitrification pathway and underpin the importance of community structure for N₂O emissions. *PLoS One* 9 (12), e114118.
- Grießmeier, V., Bremges, A., McHardy, A.C., Gescher, J., 2017. Investigation of different nitrogen reduction routes and their key microbial players in wood chip-driven denitrification beds. *Sci. Rep.* 7 (1), 17028.
- Grießmeier, V., Wienhöfer, J., Horn, H., Gescher, J., 2021. Assessing and modeling biocatalysis in field denitrification beds reveals key influencing factors for future constructions. *Water Res.* 188, 116467.
- Hassanpour, B., Giri, S., Puer, W.T., Steenhuis, T.S., Geohring, L.D., 2017. Seasonal performance of denitrifying bioreactors in the Northeastern United States: field trials. *J. Environ. Manag.* 202, 242–253.
- Hellman, M., Hubalek, V., Juhanson, J., Almstrand, R., Peura, S., Hallin, S., 2021. Substrate type determines microbial activity and community composition in bioreactors for nitrate removal by denitrification at low temperature. *Sci. Total Environ.* 755, 143023.
- Hellman, M., Valhondo, C., Martínez-Landa, L., Carrera, J., Juhanson, J., Hallin, S., 2022. Nitrogen removal capacity of microbial communities developing in compost- and woodchip-based multipurpose reactive barriers for aquifer recharge with wastewater. *Front. Microbiol.* 13.
- Henry, S., Baudoin, E., López-Gutiérrez, J.C., Martin-Laurent, F., Brauman, A., Philippot, L., 2004. Quantification of denitrifying bacteria in soils by nirK gene targeted real-time PCR. *J. Microbiol. Methods* 59 (3), 327–335.
- Henry, S., Bru, D., Stres, B., Hallet, S., Philippot, L., 2006. Quantitative detection of the nosZ gene, encoding nitrous oxide reductase, and comparison of the abundances of 16S rRNA, narG, nirK, and nosZ genes in soils. *Appl. Environ. Microbiol.* 72 (8), 5181–5189.
- Herbert, R.B., Winbjörk, H., Hellman, M., Hallin, S., 2014. Nitrogen removal and spatial distribution of denitrifier and anammox communities in a bioreactor for mine drainage treatment. *Water Research* 66 (0), 350–360.
- Herrmann, M., Wegner, C.-E., Taubert, M., Geesink, P., Lehmann, K., Yan, L., Lehmann, R., Totsche, K.U., Küsel, K., 2019. Predominance of cand. Patescibacteria in groundwater is caused by their preferential mobilization from soils and flourishing under oligotrophic conditions. *Front. Microbiol.* 10.
- Hoover, N.L., Bhandari, A., Soupir, M.L., Moorman, T.B., 2016. Woodchip denitrification bioreactors: impact of temperature and hydraulic retention time on nitrate removal. *J. Environ. Qual.* 45 (3), 803–812.
- Hosokawa, S., Kuroda, K., Narihiro, T., Aoi, Y., Ozaki, N., Ohashi, A., Kindaichi, T., 2021. Cometabolism of the superphylum Patescibacteria with anammox bacteria in a long-term freshwater anammox column reactor. *Water* 13 (2), 208.
- IPCC, 2019. N₂O emissions from managed soils, and CO₂ emissions from lime and urea application. In: Buendia, E.C., Tanabe, K.T., Kranjc, A., Jamsranjav, B., Fukuda, M., Ngarize, A., Osako, A., Pyrozhenko, Y., Shermanau, P., Federici, S. (Eds.), 2019 Refinement to the 2006 IPCC Guidelines for National Greenhouse Gas Inventories, vol. 4. IPCC, Geneva, p. 11.3. Available online at: https://www.ipcc-nggip.iges.or.jp/public/2019rrf/pdf/4_Volume4/19R_V4_Ch11_Soils_N2O_CO2.pdf. (Accessed 8 November 2023). Hergoualc'h, K., Akiyama, H., Bernoux, M., Chirinda, N., del Prado, A., Kasimir, Å., MacDonald, J. D., Ogle, S. M., Regina, K., van der Weerden, T. J., 2019.
- Jang, J., Anderson, E.L., Venterea, R.T., Sadowsky, M.J., Rosen, C.J., Feyereisen, G.W., Ishii, S., 2019. Denitrifying bacteria active in woodchip bioreactors at low-temperature conditions. *Front. Microbiol.* 10, 635.
- Jégot, A., Sørensen, S.R., Schnorr, K.M., Plauborg, F., Elsgaard, L., 2021. Temperature sensitivity and composition of nitrate-reducing microbiomes from a full-scale woodchip bioreactor treating agricultural drainage water. *Microorganisms* 9 (6).
- Jégot, A., Schnorr, K.M., Sørensen, S.R., Elsgaard, L., 2022. Isolation and characterization of psychrotolerant denitrifying bacteria for improvement of nitrate removal in woodchip bioreactors treating agricultural drainage water at low temperature. *Environ. Sci. J. Integr. Environ. Res.: Water Research & Technology* 8 (2), 396–406.
- Jones, C.M., Graf, D.R.H., Bru, D., Philippot, L., Hallin, S., 2013. The unaccounted yet abundant nitrous oxide-reducing microbial community: a potential nitrous oxide sink. *ISME J.* 7 (2), 417–426.
- Jukes, T.H., Cantor, C.R., 1969. In: Munro, H.N. (Ed.), *Academic Press*, pp. 21–132. New York.
- Kim, D.D., Han, H., Yun, T., Song, M.J., Terada, A., Laureni, M., Yoon, S., 2022. Identification of nosZ-expressing microorganisms consuming trace N₂O in microaerobic chemostat consortia dominated by an uncultured Burkholderiales. *ISME J.* 16, 2087–2098.
- Kraft, B., Tegetmeyer, H.E., Sharma, R., Klotz, M.G., Ferdelman, T.G., Hettich, R.L., Geelhoed, J.S., Strous, M., 2014. The environmental controls that govern the end product of bacterial nitrate respiration. *Science* 345 (6197), 676–679.
- Lefèvre, E., Pereyra, L.P., Hiibel, S.R., Perrault, E.M., De Long, S.K., Reardon, K.F., Pruden, A., 2013. Molecular assessment of the sensitivity of sulfate-reducing microbial communities remediating mine drainage to aerobic stress. *Water Res.* 47 (14), 5316–5325.
- Letunic, I., Bork, P., 2007. Interactive Tree of Life (iTOL): an online tool for phylogenetic tree display and annotation. *Bioinformatics* 23 (1), 127–128.
- Long, L.M., Schipper, L.A., Bruesewitz, D.A., 2011. Long-term nitrate removal in a denitrification wall. *Agric. Ecosyst. Environ.* 140 (3–4), 514–520.
- Manca, F., De Rosa, D., Reading, L.P., Rowlings, D.W., Scheer, C., Schipper, L.A., Grace, P.R., 2021. Effect of soil cap and nitrate inflow on nitrous oxide emissions from woodchip bioreactors. *Ecol. Eng.* 166, 106235.
- Martin, E.A., Davis, M.P., Moorman, T.B., Isenhardt, T.M., Soupir, M.L., 2019. Impact of hydraulic residence time on nitrate removal in pilot-scale woodchip bioreactors. *J. Environ. Manag.* 237, 424–432.
- McGuire, P.M., Dai, V.T., Walter, M.T., Reid, M.C., 2021. Labile carbon release from oxic-anoxic cycling in woodchip bioreactors enhances nitrate removal without increasing

- nitrous oxide accumulation. *Environmental Science-Water Research & Technology* 7 (12), 2357–2371.
- McGuire, P.M., Butkevich, N., Saksena, A.Y., Walter, M.T., Shapleigh, J.P., Reid, M.C., 2023. Oxidic–anoxic cycling promotes coupling between complex carbon metabolism and denitrification in woodchip bioreactors. *Environ. Microbiol.* 25 (9), 1696–1712.
- Mohan, S.B., Schmid, M., Jetten, M., Cole, J., 2004. Detection and widespread distribution of the *nrfA* gene encoding nitrite reduction to ammonia, a short circuit in the biological nitrogen cycle that competes with denitrification. *FEMS Microbiol. Ecol.* 49 (3), 433–443.
- Muyzer, G., Dewaal, E.C., Uitterlinden, A.G., 1993. Profiling of complex microbial populations by denaturing gradient gel-electrophoresis analysis of polymerase chain reaction-amplified genes coding for 16S ribosomal RNA. *Appl. Environ. Microbiol.* 59 (3), 695–700.
- Nordström, A., Hellman, M., Hallin, S., Herbert, R.B., 2021. Microbial controls on net production of nitrous oxide in a denitrifying woodchip bioreactor. *J. Environ. Qual.* 50 (1), 228–240.
- Nordström, A., Herbert, R.B., 2017. Denitrification in a low-temperature bioreactor system at two different hydraulic residence times: laboratory column studies. *Environ. Technol.* 38 (11), 1362–1375.
- Nordström, A., Herbert, R.B., 2018. Determination of major biogeochemical processes in a denitrifying woodchip bioreactor for treating mine drainage. *Ecol. Eng.* 110, 54–66.
- Parada, A.E., Needham, D.M., Fuhrman, J.A., 2016. Every base matters: assessing small subunit rRNA primers for marine microbiomes with mock communities, time series and global field samples. *Environ. Microbiol.* 18 (5), 1403–1414.
- Pedersen, A.R., 2020. **HMR: Flux Estimation with Static Chamber Data. R package version 1.0.1.** <https://CRAN.R-project.org/package=HMR>.
- Philippot, L., Andert, J., Jones, C.M., Bru, D., Hallin, S., 2011. Importance of denitrifiers lacking the genes encoding the nitrous oxide reductase for N₂O emissions from soil. *Global Change Biol.* 17 (3), 1497–1504.
- Porter, M.D., et al., 2015. Seasonal patterns in microbial community composition in denitrifying bioreactors treating subsurface agricultural drainage. *Microb. Ecol.* 70 (3), 710–723.
- Pruesse, E., Peplies, J., Glöckner, F.O., 2012. SINA: accurate high-throughput multiple sequence alignment of ribosomal RNA genes. *Bioinformatics* 28 (14), 1823–1829.
- Price, M.N., Dehal, P.S., Arkin, A.P., 2009. FastTree: computing large minimum evolution trees with profiles instead of a distance matrix. *Mol. Biol. Evol.* 26 (7), 1641–1650.
- Quince, C., Lanzen, A., Davenport, R.J., Turnbaugh, P.J., 2011. Removing noise from pyrosequenced amplicons. *BMC Bioinf.* 12 (1), 38.
- R Development Core Team, 2021. **R: A Language and Environment for Statistical Computing.** R Foundation for Statistical Computing.
- Robertson, W.D., Cherry, J.A., 1995. In-situ denitrification of septic-system nitrate using reactive porous-media barriers. - *Field Trials Ground Water* 33 (1), 99–111.
- Robertson, W.D., Vogan, J.L., Lombardo, P.S., 2008. Nitrate removal rates in a 15-year-old permeable reactive barrier treating septic system nitrate. *Ground Water Monit. Remed.* 28 (3), 65–72.
- Saghai, A., Banjeree, S., Degrune, F., Edlinger, A., Garcia-Palacios, P., Garland, G., Heijden, M.G.A., Herzog, C., Maestre, F.T., Pescador, D.S., Philippot, L., Rillig, M.C., Romdhane, S., Hallin, S., 2022. Diversity of archaea and niche preferences among putative ammonia-oxidizing Nitrososphaeria dominating across European arable soils. *Environ. Microbiol.* 24 (1), 341–356.
- Schaefer, A., Werning, K., Hoover, N., Tschirner, U., Feyereisen, G., Moorman, T.B., Howe, A.C., Soupir, M.L., 2021. Impact of flow on woodchip properties and subsidence in denitrifying bioreactors. *Agrosystems Geosciences & Environment* 4 (1).
- Schipper, L.A., Robertson, W.D., Gold, A.J., Jaynes, D.B., Cameron, S.C., 2010. Denitrifying bioreactors—An approach for reducing nitrate loads to receiving waters. *Ecol. Eng.* 36 (11), 1532–1543.
- Schipper, L.A., Vojvodić-Vuković, M., 2000. Nitrate removal from groundwater and denitrification rates in a porous treatment wall amended with sawdust. *Ecol. Eng.* 14 (3), 269–278.
- Schmid, M.C., Hooper, A.B., Klotz, M.G., Woebken, D., Lam, P., Kuypers, M.M.M., Pommerening-Roeser, A., op den Camp, H.J.M., Jetten, M.S.M., 2008. Environmental detection of octahem cytochrome c hydroxylamine/hydrazine oxidoreductase genes of aerobic and anaerobic ammonium-oxidizing bacteria. *Environ. Microbiol.* 10 (11), 3140–3149.
- Throbäck, I.N., Enwall, K., Jarvis, A., Hallin, S., 2004. Reassessing PCR primers targeting *nirS*, *nirK* and *nosZ* genes for community surveys of denitrifying bacteria with DGGE. *FEMS Microbiol. Ecol.* 49 (3), 401–417.
- Tian, L., Cai, Y., Akiyama, H., 2019. A review of indirect N₂O emission factors from agricultural nitrogen leaching and runoff to update of the default IPCC values. *Environ. Pollut.* 245, 300–306.
- Wang, J.L., Chu, L.B., 2016. Biological nitrate removal from water and wastewater by solid-phase denitrification process. *Biotechnol. Adv.* 34 (6), 1103–1112.
- Warneke, S., Schipper, L.A., Bruesewitz, D.A., McDonald, I., Cameron, S., 2011. Rates, controls and potential adverse effects of nitrate removal in a denitrification bed. *Ecol. Eng.* 37 (3), 511–522.
- Welsh, A., Chee-Sanford, J.C., Connor, L.M., Löffler, F.E., Sanford, R.A., 2014. Refined *nrfA* phylogeny improves PCR-based *nrfA* gene detection. *Appl. Environ. Microbiol.* 80 (7), 2110–2119.